COMPDYN 2011
III ECCOMAS Thematic Conference on
Computational Methods in Structural Dynamics and Earthquake Engineering
M. Papadrakakis, M. Fragiadakis, V. Plevris (eds.)
Corfu, Greece, 25–28 May 2011

NONLINEAR VISCOELASTIC ANALYSIS OF A PNEUMATIC 2D STRUCTURE INTERPOSED BETWEEN A COUPLE OF RIGID MOVING PLANES

Andrea De Simone[1], Angelo Luongo[2]

[1]Università degli Studi dell'Aquila
Dipartimento di Ingegneria delle Strutture, delle Acque e del Terreno
Via Giovanni Falcone 25, 67100 Coppito (AQ), Italy
andrea.desimone@univaq.it

[2]Università degli Studi dell'Aquila
Dipartimento di Ingegneria delle Strutture, delle Acque e del Terreno
Via Giovanni Falcone 25, 67100 Coppito (AQ) , Italy
angelo.luongo@univaq.it

Keywords: Balloon Mechanics, Contact Problem, Balloon Squeezing, Visco-elasticity, Fender-ship Model.

Abstract. *A nonlinear planar model of visco-elastic balloon, interposed between a couple of moving rigid bodies, is formulated. The pneumatic structure is modeled as an initially circular cable, pre-stressed by an internal pressure, and constrained to remain in a planar domain. External pressure is assumed to be zero. The pushing bodies are modeled as a couple of frictionless rigid parallel bars, approaching each other normally, and causing squeezing of the pneumatic body. Motion is assumed slow, in such a way any inertial effects are negligible. Both cases of long and short bars are considered, the latter entailing the possibility of puncture of the deformable body. A thermoplastic polyurethane material behavior is considered, and proper constitutive relationships adopted. Several models are formulated, which differ for constitutive laws (inextensible, elastic, linearly or non linearly visco-elastic) and/or for kinematic analysis (small strains and displacements or finite kinematics). The governing mixed differential-algebraic equations are analytically or numerically integrated for several impressed motion time-histories and the main features of the phenomenon are investigated.*

1 INTRODUCTION

Pneumatic structures have many applications in different technical fields. Often, they consist in balloons interposed between bodies of higher stiffness, that cause their squeezing or puncture. Examples are given by fender-devices, gaskets, balloons for bulkheads control, blood vessels and angioplastic balloons. Fender-devices are used in nautical, as peer-fenders, ship-fenders and rollers; pressurized gaskets are interposed between bodies in contacts; ballons are used to lift-up bulkheads, to create artificial rapids for rafting; balloons are also extensively used for biomedical applications, e.g. to free narrowed arteries obstructed by cholesterol and fats in general.

In all these application, it is of interest to predict the evolution in time of the geometry of the balloon, of its stress, its strain and its internal pressure. Of course, the response of the balloon depends on several causes: (a) the stiffness and geometry of the in-contact bodies, (b) the type of friction at the contact, (c) the law of relative motion of the bodies, (d) the geometry of the balloon, (e) the constitutive law of the material of which the balloon is made. Here, a first attempt is made to approach the problem in a simple way, by using simple models, leading to analytical or semi-analytic solutions. The goal is to gain insights into the physics of the phenomenon, and to highlight the implications of different levels of approximation in the analysis.

A long cylindrical balloon under internal pressure is considered, interposed between two rigid planar surfaces, slowly approaching each other normally. External pressure is assumed zero. By ignoring boundary effects, the problem is studied as planar, in the plane orthogonal to the cylinder axis. The structural model consists therefore in an initially circular cable, pre-stressed by an internal pressure, squeezed by two rigid and parallel bars, assumed frictionless [1]. Due to the prescribed motion of the bars, quasi-static variations of geometry, stress, and internal pressure occur. The configuration history is sketched in Fig 1, for both cases of 'long' (Fig 1a) and 'short' (Fig 1b) bars. Contact initially occurs at one point on each bar (phase I in Fig 1a,b), then it extends over a segment during the loading process (phases II in Fig 1a,b), while the free part of the cable keeps its circular shape, with modified unknown radius. These two phases are common to both kind of bars. If the bar are long, however, the process ends with a complete adhesion of cable to the bodies (phase III in Fig 1a). If the bars are short, in contrast, a critical configuration is observed (phases III in Fig 1b), in which a part of the cable is adherent to the bars for their entire length, but a remaining part is still free. Then, a partial puncture of the deformable body occurs (phase IV in Fig 1b) ending with a complete puncture (phase V in Fig 1b).

Different models are adopted for the balloon material behavior, namely (1) inextensible, (2) elastic, (3) linear visco-elastic, (4) large-strain visco-elastic, (5) fully non-linear visco-elastic. Models (3)-(5) differ in kinematic description (small strains and displacements regime, or finite kinematics) and in stress-strain-rate relationships (linear or nonlinear). In model (5), a thermoplastic polyurethane material is considered, and a properly simplified constitutive relationship adopted, deduced by the literature [2,3]. The five models are aimed to highlight the influence of the constitutive law and large displacements and strain on the overall response. For all the models considered, the formulation is illustrated, and the solution, analytical or numerical, given. Numerical results, relevant to different loading time-histories, are finally displayed and commented.

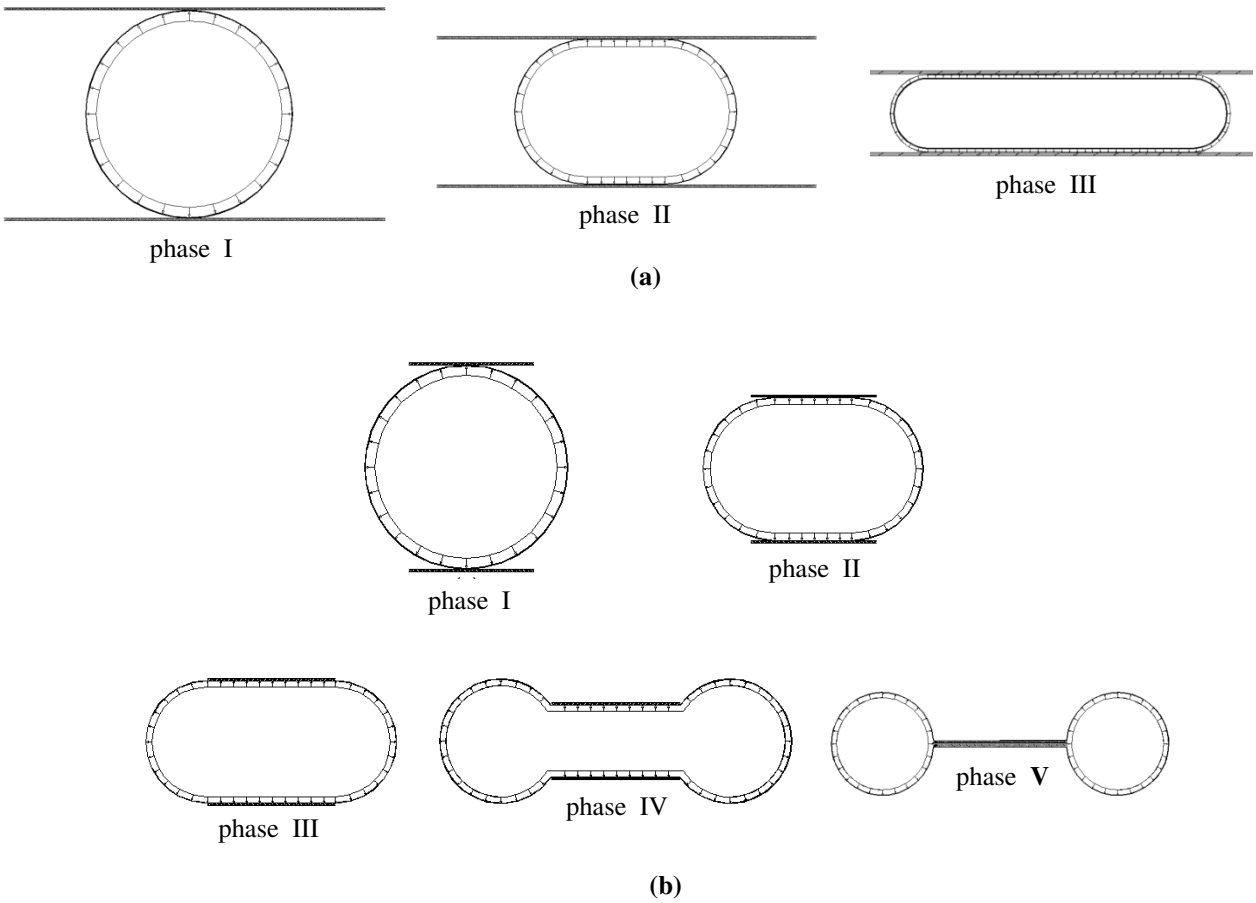

Figure 1: Evolution of the cable configuration: (a) long bars: (I) initial contact, (II) partial contact, (III) advanced configuration (close to total adhesion); (b) short bars: (I) initial contact, (II) partial contact, (III) critical configuration, (IV) punctured configuration, (V) final configuration (totally punctured).

2 MODEL FORMULATION

2.1 State-variables, pre- and post-critical states

The physical system is made of two components, the cable and the insufflated air. Its mechanical state is defined by quantities able to describe (a) the actual shape of the system (by configuration variables), (b) the state of strain (by extensive variables) and (c) the state of stress (by dual intensive variables). As it will be explained soon, since the cable is made of rectilinear and circular parts, two configuration variables are sufficient to describe the geometry. However, one of them must be taken as control parameter for the loading process, so that just one geometrical variable is unknown; it is convenient to take it as the radius R of the circular part. On the other hand, the state of the air is defined by its pressure P and by the volume V instantaneously included in the cable. The state of the cable is determined by the stress T and the strain ε, this latter measured with respect to a reference (or *initial*) configuration $\mathcal{C}_I$. Due to geometry, both these quantities are constant along the cable. By summarizing, the state is described by five scalar quantities (state-variables), $\mathbf{x} := (R, P, V, T, \varepsilon)$, all depending on time.

The state of first-contact between cable and rods (phase I in Fig 1) is taken as initial configuration. Here $\mathbf{x}_I := (R_I, P_I, V_I, T_I, \varepsilon_I)$ are assumed to be known quantities. Their evaluation, of

course, calls for solving a *pre-contact evolution problem*, in which the circular cable is free. This transformation leads the body from its natural state to the initial state, as a consequence of its own visco-elastic properties.

By accounting for the double symmetry of the system, only a quarter of the cable is considered, as shown in Fig 2, for the two cases of long bars (Fig 2a,b) and short bars (Fig 2c,d). In the initial configuration (Fig 2a,c) the cable is circular, of center O, and delimited by the (material) contact point A and the symmetry point C; the volume subtended by this arc is $V_I = \pi R_I^2 / 4$. In the actual (or *varied*) configuration $\mathcal{C}_V$ (Fig 2b,c), a third point B is of interest, which separates the contact portion of cable (AB segment) from the circular part (BC arc). The projection of B on the horizontal symmetry axis is the new center O' of the arc. The varied configuration is determined once the radius R and the angle $\theta = A\hat{O}B$ are known. Although R coincides with the (assigned) semi-distance a between the two rods, it appears computationally more convenient to take the angle θ, instead of R, as control parameter for the loading process, by leaving to R the meaning of configuration variable. This state, that also occurs for short bars, will be referred to as *pre-critical.*

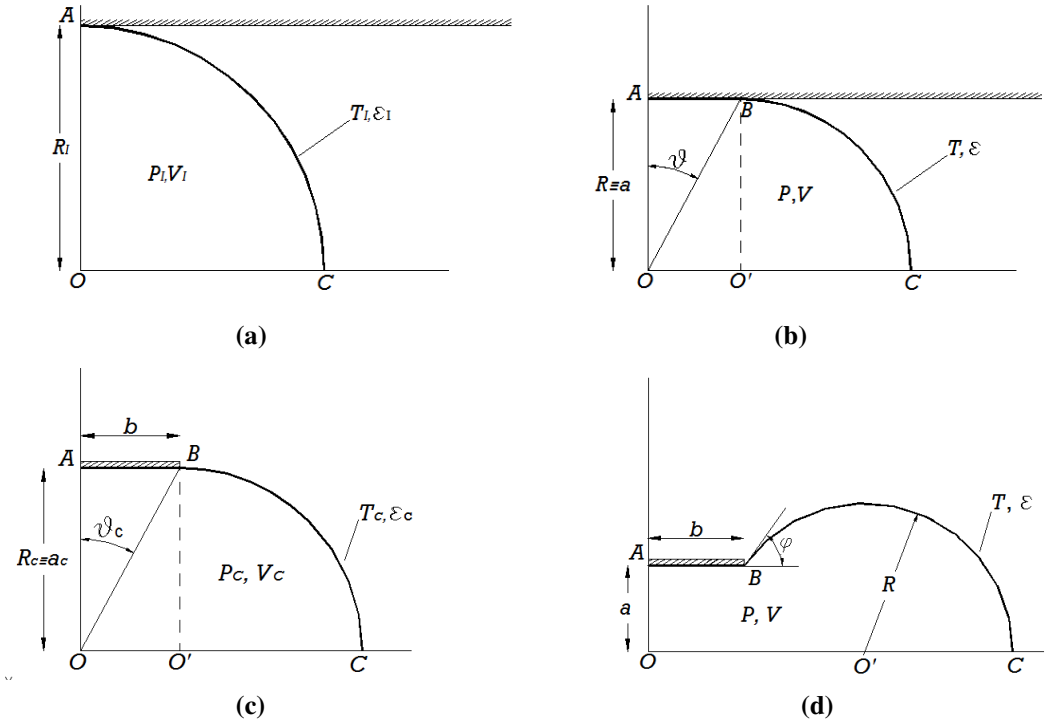

Figure 2: Configurations and state variables for long (a,b) and short (c,d) bars: (a) initial state; (b) actual state; (c) critical state; (d) actual (post-critical) configuration. θ, φ are control parameters.

If the bars are short, the system experiences a *critical state* $\mathcal{C}_C$ in which the contact point B coincides with an end of the bar (Fig 2c); in this configuration the quantities previously introduced assume the values $\mathbf{x}_C := (R_C, P_C, V_C, T_C, \varepsilon_C)$. A further approach between the bars causes the new geometrical structure of Fig 2d (punctured configuration). In order to describe how the phenomenon evolves, the new control parameter φ is chosen, which is the angle that the tangent at the circular arc at point B forms with the horizontal axis. The center of the arc, O', is no more the projection of B, and therefore a and R are no more coincident, but $a = R\cos\varphi$.

In this phase, the state-variables will be still denoted by $\mathbf{x} := (R, P, V, T, \varepsilon)$, but the state will be referred to as *post-critical*. The history of these quantities, as well as the instant at which the system reaches the critical configuration, now depends on the bar semi-length b.

2.2 Governing equations

The formulation of the problem calls for establishing balance equations, geometric compatibility and constitutive equations. The balance equation expresses the equilibrium of an elementary material element belonging to the circular portion of the cable, namely:

$$T = PR \tag{1}$$

Equilibrium of the rectilinear part, indeed, is guaranteed by the fact that $T = \text{const}$ along the cable. Indeed, the internal pressure is balanced by the reactions normal to the contact, while no tangential forces act on the cable, since friction has been neglected.
As regards the constitutive laws, air is assumed to behave as perfect gas, and transformations are considered isothermal, for which:

$$PV = P_I V_I \tag{2}$$

The cable behavior, instead, is modeled in several ways. In the more general, visco-elastic case, the constitutive law assumes the form:

$$f(T, \dot{T}, \varepsilon, \dot{\varepsilon}) = 0 \tag{3}$$

where the dot denotes time-differentiation, and the initial conditions $T(0) = T_I$, $\varepsilon(0) = \varepsilon_I$ are prescribed.
The kinematics of the system requires writing two additional compatibility equations, expressing the two extensive variables, V, ε, in terms of the unique configuration variable R. They will be named the *volumetric* and *extensional* compatibility equations, respectively. Concerning volume, elementary calculations relevant to the shape assumed by the cable in Fig 2b,d, lead to:

$$V = \begin{cases} R^2\left(\tan\theta + \dfrac{\pi}{4}\right) & \text{in pre-critical phase} \\ \dfrac{R^2}{4}\left(\sin 2\varphi + \pi + 2\varphi\right) + bR\cos\varphi & \text{in post-critical phase} \end{cases} \tag{4}$$

where, of course, the post-critical phase exists only if the bars are short. Concerning the strain, and defining it as the specific elongation $\varepsilon := (l / l_I) - 1$, with l and l_I being the total length of the cable in the actual and initial configuration, it follows, that:

$$\varepsilon = \begin{cases} \dfrac{R}{R_I}\left(1 + \dfrac{2}{\pi}\tan\theta\right) - 1 & \text{in pre-critical phase} \\ \dfrac{R}{R_I}\left(1 + \dfrac{2}{\pi}\varphi\right) + \dfrac{2b}{\pi R_I} - 1 & \text{in post-critical phase} \end{cases} \tag{5}$$

In the critical state is: $\tan\theta = b / R, \varphi = 0$, so that both the alternative expressions in Eqs (4) and (5) furnish $\varepsilon_C = R / R_I + (2b) / (\pi R_I)$ and $V_C = bR + \pi R^2 / 4$.

3 SPECIALIZED CONSTITUTIVE MODELS

The governing equations (1)-(5) are specialized ahead to different constitutive models of cable. Non-dimensional quantities are used, according to the following definitions:

$$\begin{gathered} p := P / P_1, \quad \tau = T / T_1, \quad v := V / V_1, \quad r := R / R_1 \\ \alpha = a / R_1, \quad \beta = b / R_1 \end{gathered} \tag{6}$$

in which $T_1 = P_1 R_1$ holds, since $\mathcal{C}_1$ is equilibrated.

3.1 Inextensible cable

The simplest model of material behavior is the inextensible model. Accordingly, the cable is considered perfectly flexible, but axially indeformable. In this case, no a constitutive law like Eq (3) exists, since the stress T assumes a reactive character. On the other hand, compatibility requires $\varepsilon = 0$, so that Eq (5) simplifies. Therefore, the relevant mechanical problem is governed by four equations in four unknowns. By using non-dimensional quantities, they read:

$$\tau = pr, \quad pv = 1, \quad v = \begin{cases} r^2\left(1+\dfrac{4}{\pi}\tan\theta\right) \\ r^2\left(1+\dfrac{2}{\pi}\varphi+\dfrac{1}{\pi}\sin 2\varphi\right)+\dfrac{4}{\pi}\beta r\cos\varphi \end{cases}, \quad \begin{cases} r\left(1+\dfrac{2}{\pi}\tan\theta\right)=1 \\ r\left(1+\dfrac{2}{\pi}\varphi\right)+\dfrac{2}{\pi}\beta=1 \end{cases} \tag{7}$$

in the pre-critical and post-critical phase, respectively.

3.2 Elastic cable

An improved model accounts for elasticity of the cable. By assuming that the body obeys to the Hooke law, and considering the initial stress, the constitutive relationship reads:

$$T = T_1 + EA_1\varepsilon \tag{8}$$

where EA_1 is the axial stiffness evaluated at $\mathcal{C}_1$. In non-dimensional form, the elastic problem (1)-(5) reads:

$$\tau = pr, \quad pv = 1, \quad \tau = 1 + k\varepsilon,$$

$$v = \begin{cases} r^2\left(1+\dfrac{4}{\pi}\tan\theta\right) \\ r^2\left(1+\dfrac{2}{\pi}\varphi+\dfrac{1}{\pi}\sin 2\varphi\right)+\dfrac{4}{\pi}\beta r\cos\varphi \end{cases}, \quad \varepsilon = \begin{cases} r\left(1+\dfrac{2}{\pi}\tan\theta\right)-1 \\ (r+2\beta)\left(1+\dfrac{2}{\pi}\varphi\right)-1 \end{cases} \tag{9}$$

in the two phases, respectively. In Eqs (9) the following non-dimensional elastic stiffness has been introduced:

$$k := EA_1 / T_1 \tag{10}$$

3.3 Linear visco-elastic cable

To account for slow-time effects and for internal energy dissipation of the cable, a visco-elastic constitutive model must be used. As a first, simplest approach to the problem, the well-known *linear* standard model (also called 'three parameter model', Fig 3) is adopted.

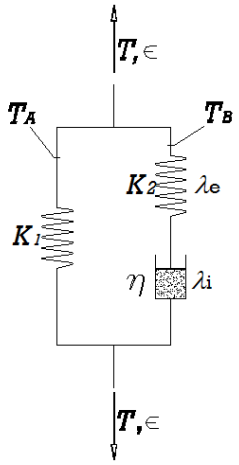

Figure 3: Standard visco-elastic model

The relevant constitutive relationship is:

$$\begin{cases} \dot{T} + \dfrac{K_2}{\eta} T = (K_1 + K_2)\dot{\varepsilon} + \dfrac{K_1 K_2}{\eta} \varepsilon \\ T(0) = T_I, \quad \varepsilon(0) = \varepsilon_I \end{cases} \tag{11}$$

where K_1, K_2, are elastic moduli, and η a viscosity coefficient. In non-dimensional form, it reads:

$$\begin{cases} \dot{\tau} + \tau = (k_1 + k_2)\dot{\varepsilon} + k_1 \varepsilon \\ \tau(0) = 1, \quad \varepsilon(0) = \varepsilon_I \end{cases} \tag{12}$$

where:

$$\tilde{t} := (K_2 / \eta)t, \quad k_1 := K_1 / T_I, \quad k_2 := K_2 / T_I \tag{13}$$

have been introduced, and where the dot now denotes differentiation with respect the non-dimensional time $\tilde{t}$ (tilde dropped ahead). The visco-elastic problem for the system is therefore governed by:

$$\tau = pr, \quad pv = 1, \quad v = \begin{cases} r^2 \left(1 + \dfrac{4}{\pi}\tan\theta\right) \\ r^2 \left(1 + \dfrac{2}{\pi}\varphi + \dfrac{1}{\pi}\sin 2\varphi\right) + \dfrac{4}{\pi}\beta r \cos\varphi \end{cases}, \quad \varepsilon = \begin{cases} r\left(1 + \dfrac{2}{\pi}\tan\theta\right) - 1 \\ (r + 2\beta)\left(1 + \dfrac{2}{\pi}\varphi\right) - 1 \end{cases} \tag{14}$$

$$\dot{\tau} + \tau = (k_1 + k_2)\dot{\varepsilon} + k_1 \varepsilon, \quad \tau(0) = 1, \quad \varepsilon(0) = \varepsilon_I$$

It is therefore a mixed differential-algebraic problem, whose solution calls for a numeric integration. It can be recast in the matrix form:

$$\begin{cases} \mathbf{A}(\mathbf{y}(t))\dot{\mathbf{y}}(t) + \mathbf{B}(\mathbf{y}(t))\mathbf{y}(t) = \mathbf{f}(t) \\ \mathbf{y}(0) = \mathbf{y}_0 \end{cases} \tag{15}$$

where $\mathbf{A}$ and $\mathbf{B}$ are 6×6 matrices, $\mathbf{y} = (\mathbf{x};\theta)$ or $\mathbf{y} = (\mathbf{x};\varphi)$ is an extended 6-vector of state variables, including the control parameter, and $\mathbf{f}(t) = (1,1,0,-1,0;f(t))$ is a 6-vector of know-terms, in which $f(t)$ denotes the impressed time-history for $\theta(t)$ or $\varphi(t)$. Moreover $\mathbf{y}_0 = (r_I, p_I, v_I, \tau_I, \varepsilon_I; f(0))$. Equations (15) have been integrated by using a solver for singular and sparse matrices.

3.4 Large strain visco-elastic cable

An enhanced visco-elastic model is introduced, in which large strains are accounted for. The stretch $\lambda := 1+\varepsilon$ (whose logarithm is known as the 'true strain') instead of the (engineering) elongation ε, is used as the strain measure, since this latter is not additive in finite kinematics[1]. Reference is made again to the three-parameter model of Fig 3, in which *A* is the elastic part and *B* the visco-elastic part. Compatibility for the two parts requires $\lambda_A = \lambda_B =: \lambda$, while compatibility for part *B* calls for $\lambda = \lambda_i\lambda_e$, where $\lambda_{i,e}$ are the stretches of the in-series inelastic and elastic devices, respectively. Equilibrium requires that $T = T_A + T_B$ and $T_i = T_e =: T_B$. By still assuming linear constitutive laws for the single devices, namely:

$$T_A = K_1(\lambda - 1), \quad T_B = K_2(\lambda_e - 1), \quad T_B = \eta\dot{\lambda}_i \tag{16}$$

the following nonlinear stress-strain law is finally derived, with relevant initial conditions:

$$\begin{cases} \lambda\dot{T} - (K_1 + K_2 + T)\dot{\lambda} + \dfrac{K_2}{\eta}\left[T - K_1(\lambda - 1)\right]\left[1 - \dfrac{K_1}{K_2}(\lambda - 1) + \dfrac{T}{K_2}\right]^2 = 0 \\ T(0) = T_I, \quad \lambda(0) = \lambda_I \end{cases} \tag{17}$$

It should be noted that, for small strain and $T << K_2$, the squared bracket in Eq (17) tends to 1, so that Eq. (11) is recovered. In nondimensional variables, Eq. (17) reads:

$$\begin{cases} \lambda\dot{\tau} - (k_1 + k_2 + \tau)\dot{\lambda} + \left[\tau - k_1(\lambda - 1)\right]\left[1 - \dfrac{k_1}{k_2}(\lambda - 1) + \dfrac{\tau}{k_2}\right]^2 = 0 \\ \tau(0) = \tau_I, \quad \lambda(0) = \lambda_I \end{cases} \tag{18}$$

The visco-elastic problem for the large-strain cable model is therefore governed by the following set of equations:

---

[1] Indeed, if $\Delta l_1, \Delta l_2$ are two successive deformations of a segment of initial length l, then the final strain $\dfrac{\Delta l_1 + \Delta l_2}{l}$ differs from the sum of the two strains: $\varepsilon_1 \dfrac{\Delta l_1}{l}, \varepsilon_2 = \dfrac{\Delta l_2}{l + \Delta l_1}$. In contrast, since $\lambda = \dfrac{l + \Delta l_1 + \Delta l_2}{l}$, $\lambda_1 = \dfrac{l + \Delta l_1}{l}$, $\lambda_2 = \dfrac{l + \Delta l_1 + \Delta l_2}{l + \Delta l_1}$, then $\lambda = \lambda_1\lambda_2$.

$$\tau = pr, \quad pv = 1, \quad v = \begin{cases} r^2\left(1+\frac{4}{\pi}\tan\theta\right) \\ r^2\left(1+\frac{2}{\pi}\varphi+\frac{1}{\pi}\sin 2\varphi\right)+\frac{4}{\pi}\beta r\cos\varphi \end{cases}, \quad \varepsilon = \begin{cases} r\left(1+\frac{2}{\pi}\tan\theta\right)-1 \\ (r+2\beta)\left(1+\frac{2}{\pi}\varphi\right)-1 \end{cases} \tag{19}$$

$$\lambda\dot{\tau}-(k_1+k_2+\tau)\dot{\lambda}+\left[\tau-k_1(\lambda-1)\right]\left[1-\frac{k_1}{k_2}(\lambda-1)+\frac{\tau}{k_2}\right]^2=0, \quad \tau(0)=\tau_1, \quad \lambda(0)=\lambda_1$$

The whole system is then rearranged as in Eqs (15), to be numerically integrated.

3.5 Fully-nonlinear visco-elastic cable

Although the previous model accounts for large strains, the constitutive laws (16) of the single components are still linear. To formulate a fully-nonlinear visco-elastic model (i.e. large-strain and mechanically nonlinear), it needs to more accurately describe the stress-strain-rate law. Here, reference is made to a thermoplastic polyurethane material, for which a proper 3D-constitutive law has been proposed in [2], still based on the model of Fig. 3. It involves all the eigenvalues $\lambda_1, \lambda_2, \lambda_3$ of the deformation gradient **F**. To reduce the model to 1D, two hypotheses were introduced: (a) *each* parts *A* and *B* are incompressible, and (b) the material is transversally isotropic, these entailing $\lambda_2 = \lambda_3 = \pm 1/\sqrt{\lambda}$, with $\lambda := \lambda_1$ the longitudinal stretch. Although hypothesis (a) is quite strong (since isochoricity is more likely to hold on the two parts as a whole, rather than separately), it has been introduced here to keep the model the simplest possible. Based on this approximations, the following five-parameter visco-elastic, 1D-model were obtained in [1] (quite involved details are omitted here):

$$T_A = c_1\left(\lambda^2-\frac{1}{\lambda}\right), \quad T_B = c_2\frac{\ln\lambda_e}{\lambda_e}, \quad T_B = c_3\left(\lambda_e\sqrt{1+\frac{2}{\lambda_e^3}}-1\right)^{c_4}\left(\frac{\dot{\lambda}_i}{\lambda_i}\right)^{c_5} \tag{20}$$

in which c_i are constant materials. By using compatibility and equilibrium as in the previous model, the final constitutive equation was derived. Together with Eqs ($19_{1\text{-}4}$), they govern the fully-nonlinear visco-elastic problem for the cable.

4 PRELIMINARY NUMERICAL RESULTS

The simplest inextensible and elastic models, governed by the algebraic Eqs (7) and (9), respectively, admit a closed-form solution, which is reported in the Appendix. In contrast, the mixed algebraic differential equations, governing all the visco-elastic models, call for numerical integrations. A sample numerical integration is shown here, in order to illustrate a typical time-history of a balloon (Fig 4). Three models have been considered, and the relevant results compared, namely elastic (*E*), linear visco-elastic (*LVE*) and fully nonlinear viscoelastic (*NLVE*). A fourth model, the large-strain visco-elastic, was disregarded, since it gave results very similar to the linear one. Figure 4 shows, for the three models, the strain (Fig 4a) and the stress (Fig 4b) time-histories. When $t < t_0$, the cable is at rest in its natural (unstressed, unstrained) configuration. At $t = t_0$ an internal pressure is instantaneously applied, by insufflating air, so that the cable undergoes the strain ε_0 and the tension T_0. It should be noted that these state-variables relevant to *NLVE* differ from those relevant to *E* and *LVE*, due to the dif-

ferent elastic law adopted for the former. With the air-flow stopped, a time-interval $[t_0, t_1]$ is waited, in which, due to viscosity, the strain increases, while the stress decreases. In contrast, strain and stress remain constant in the elastic model. At the instant t_1, two (long) bars are juxtaposed to the balloon, touching it each in a single point, and a constant-rate motion approach is imposed to them. Both strain and stress decrease, up the critical configuration is reached at a point C, at an instant t_C which is different for each model. After that, the constant-rate motion is continued for an additional time interval, sufficient to move the system far from the critical condition. Then, at point P, a pulsating bar movement is started, of amplitude such that the balloon remains in post-critical phase. A remarkable different behavior is also appreciated in this phase for the three models.

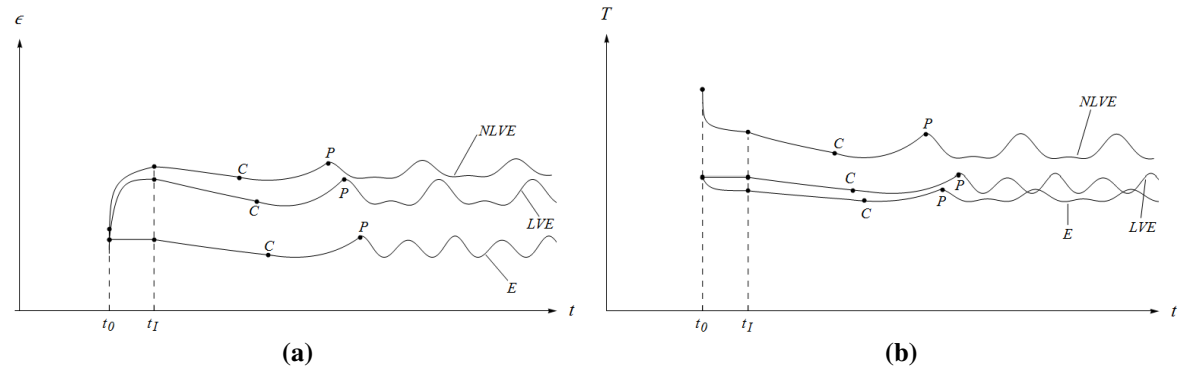

Figure 4: Time-histories of (a) strain and (b) stress; *E*:elastic, *LVC*: linear visco-elastic, *NLVE*: nonlinear visco-elastic; t_1 start of the constant-rate motion; *C*: critical point; *P*: start of the pulsating motion.

5 CONCLUSIONS

A nonlinear planar model of visco-elastic balloon, interposed between two moving rigid bars, has been formulated. The problem has been found to be governed by five algebraic-ode equations in five state-variables (radius, strain, volume, stress, internal pressure), expressing equilibrium, compatibility and stress-strain-rate relationships. The distance between the two bars (or an equivalent geometrical magnitude) is taken as loading parameter, and an arbitrarily selected time-history, assigned. According to the ratio between the radius of the balloon and the length of the bars, a one-phase evolution problem (only squeezing, for long bars) or a two-phases evolution problems (squeezing and puncture, for short bars), occur. Five specific models have been derived, of increasing complexity: inextensible, linearly elastic, linear visco-elastic, large-strain visco-elastic, fully-nonlinear visco-elastic. Preliminary analytical and numerical results have been obtained, comparing the models for a sample time-history. More extended parametric analysis will be presented at the conference.

REFERENCES

[1] A. De Simone, A non linear viscoelastic pneumatic 2D structure interposed between a couple of rigid moving surfaces, University of L'Aquila, Phd Thesis, 2010.

[2] H.J. Qi, M.C. Boyce, Stress-strain behavior of thermoplastic polyurethan. *Mechanics of materials*, 37, 817-839, 2005.

[3] McCrum N.G., Buckley C.P. and Bucknall C.B., *Principles of Polymer Engineering*. Oxford University Press, 1997.

APPENDIX: Solution to the inextensible and elastic models

Equations (7), relevant to the inextensible model, admit a unique solution, that can be obtained in closed-form. It reads:

$$r=\frac{\pi}{\pi+2\tan\theta},\quad v=\frac{\pi(4\tan\theta+\pi)}{(2\tan\theta+\pi)^2},\quad p=\frac{(2\tan\theta+\pi)^2}{\pi(4\tan\theta+\pi)},\quad \tau=1-\frac{2}{4+\pi\cot\theta} \tag{21}$$

in the pre-critical phase, and:

$$\begin{gathered} r=\frac{\pi-2\beta}{\pi+2\varphi},\quad v=\frac{(\pi-2\beta)\left(4\beta(\pi+2\varphi)\cos\varphi+(\pi-2\beta)(\pi+2\varphi+\sin 2\varphi)\right)}{\pi(\pi+2\varphi)^2}, \\ p=\frac{\pi(\pi+2\varphi)^2}{(\pi-2\beta)\left(4\beta(\pi+2\varphi)\cos\varphi+(\pi-2\beta)(\pi+2\varphi+\sin 2\varphi)\right)},\quad \tau=\frac{\pi(\pi+2\varphi)}{4\beta(\pi+2\varphi)\cos\varphi+(\pi-2\beta)(\pi+2\varphi+\sin 2\varphi)} \end{gathered} \tag{22}$$

in the post-critical phase.

Equations (9), relevant to the elastic model, can be solved analytically as well. Two distinct solutions were found; one of them, however, had to be disregarded, since physically not admissible ($\tau<0$)(see [1]). The admissible solution, instead, is:

$$\begin{gathered} \tau=\frac{1}{2}\left(1-k+\frac{\cos\theta\sqrt{\pi+4\tan\theta}\sqrt{(1+k)^2\pi+4\left(1+k^2\right)\tan\theta}}{\pi\cos\theta+4\sin\theta}\right), \\ p=\frac{\left(1+k^2\right)\pi+4\left(1+(k-1)k\right)\tan\theta-(k-1)\sqrt{\pi+4\tan\theta}\sqrt{(1+k)^2\pi+4\left(1+k^2\right)\tan\theta}}{2\pi}, \\ \varepsilon=\frac{1}{2}\left(-1+\frac{-1+\sqrt{\frac{(1+k)^2\pi+4\left(1+k^2\right)\tan\theta}{\pi+4\tan\theta}}}{k}\right), \\ v=\frac{\pi\left(\left(1+k^2\right)\pi+4\left(1+(k-1)k\right)\tan\theta+(k-1)\sqrt{\pi+4\tan\theta}\sqrt{(1+k)^2\pi+4\left(1+k^2\right)\tan\theta}\right)}{2k^2(\pi+2\tan\theta)^2}, \\ r=\frac{\pi\left(-1+k+\sqrt{\frac{(1+k)^2\pi+4\left(1+k^2\right)\tan\theta}{\pi+4\tan\theta}}\right)}{2k(\pi+2\tan\theta)} \end{gathered} \tag{23}$$

in the pre-critical phase, and**:**

$$\begin{gathered} \tau=\frac{\beta(\pi+2\varphi)-2\beta(\pi+2\varphi)\cos\varphi+\beta\sin 2\varphi+\frac{1}{2}A}{\pi(\pi+2\varphi+\sin 2\varphi)}, \\ p=\frac{1}{\pi^3-8\pi\beta^2\cos\varphi}\left(\pi^3+2\pi^2\varphi+2\beta^2\pi(1-2\cos\varphi)+2\beta^2(2\varphi-4\varphi\cos\varphi+\sin 2\varphi)+\beta A\right), \\ \varepsilon=\frac{(\beta-\pi)(\pi+2\varphi)-2\beta(\pi+2\varphi)\cos\varphi+(\beta-\pi)\sin 2\varphi+\frac{1}{2}A}{\pi(\pi+2\varphi+\sin 2\varphi)}, \\ v=\frac{1}{\pi(\pi+2\varphi)^2}\left(\pi^3+2\pi^2\varphi+2\beta^2\pi(1-2\cos\varphi)+2\beta^2(2\varphi-4\varphi\cos\varphi+\sin 2\varphi)-\beta A\right), \\ r=\frac{1}{(\pi+2\varphi)(\pi+2\varphi+\sin 2\varphi)}\left(-\beta\pi(1+2\cos\varphi)-2\beta(\varphi+\cos\varphi(2\varphi+\sin\varphi))+\frac{1}{2}A\right) \end{gathered} \tag{24}$$

in the post-critical phase, where the following constant has been defined:

$$A=\sqrt{4(\pi+2\varphi)\left(\pi^2-8\beta^2\cos\varphi\right)(\pi+2\varphi+\sin 2\varphi)+4\beta^2\left((\pi+2\varphi)(1+2\cos\varphi)+\sin 2\varphi\right)^2} \tag{25}$$